

How well does nonrelativistic QCD factorization work at next-to-leading order?

Nora Brambilla^{1,2,3}, Mathias Butenschoen⁴, and Xiang-Peng Wang¹

¹Technical University of Munich, TUM School of Natural Sciences, Physics Department,
James-Franck-Strasse 1, 85748 Garching, Germany

²Technical University of Munich, Institute for Advanced Study,
Lichtenbergstrasse 2a, 85748 Garching, Germany

³Technical University of Munich, Munich Data Science Institute,
Walther-von-Dyck-Strasse 10, 85748 Garching, Germany

⁴II. Institut für Theoretische Physik, Universität Hamburg,
Luruper Chaussee 149, 22761 Hamburg, Germany

November 26, 2024

Abstract

We perform a thorough investigation of the universality of the long distance matrix elements (LDMEs) of nonrelativistic QCD factorization based on a next-to-leading order (NLO) fit of J/ψ color octet (CO) LDMEs to high transverse momentum p_T J/ψ and η_c production data at the LHC. We thereby apply a novel fit-and-predict procedure to systematically take into account scale variations, and predict various observables never studied in this context before. In particular, the LDMEs can well describe J/ψ hadroproduction up to the highest measured values of p_T , as well as $\Upsilon(nS)$ production via potential NRQCD based relations. Furthermore, J/ψ production in $\gamma\gamma$ and γp collisions is surprisingly reproduced down to $p_T = 1$ GeV, as long as the region of large inelasticity z is excluded, which may be of significance in future quarkonium studies, in particular at the EIC and the high-luminosity LHC. In addition, our summary reveals an interesting pattern as to which observables still evade a consistent description.

1 Introduction and overview

The hierarchy of energy scales $m_Q \gg m_Q v \gg m_Q v^2$ makes heavy quarkonium production an ideal laboratory to study both the perturbative and nonperturbative aspects of QCD. Here, m_Q stands for the heavy quark mass and v for the relative velocity of the heavy quark and antiquark in the rest frame of the quarkonium. The most prominent approach to describe quarkonium production and decay is via non-relativistic QCD (NRQCD) [1]. This is an effective field theory that comes with a conjectured factorization formula, according to which a quarkonium, H , production cross section factorizes into perturbatively calculable short-distance coefficients (SDCs) and universal non-perturbative long-distance matrix elements (LDMEs) $\langle \mathcal{O}^H(n) \rangle$, where $n = {}^{2S+1}L_J^{[1/8]}$ denotes an intermediate color singlet ($^{[1]}$, CS) or octet ($^{[8]}$, CO) heavy quark-antiquark state with spin S , orbital angular momentum L and total angular momentum J . NRQCD predicts the LDMEs to scale with certain powers of v^2 via velocity scaling rules [2]. These rules predict the leading (next-to-leading) v^2 contributions to stem for $\psi(nS)$ and $\Upsilon(nS)$ production from $n = {}^3S_1^{[1]}$ (${}^1S_0^{[8]}$, ${}^3S_1^{[8]}$, ${}^3P_J^{[8]}$) and for η_c production from $n = {}^1S_0^{[1]}$ (${}^3S_1^{[8]}$, ${}^1S_0^{[8]}$, ${}^1P_1^{[8]}$). The LDMEs are, however, not all independent. Up to corrections of order v^2 , the LDMEs of J/ψ and η_c are mutually related via heavy quark spin symmetry (HQSS) [1], and the various $\psi(nS)$ and $\Upsilon(nS)$ LDMEs by relations [3, 4] based on potential NRQCD (pNRQCD) [5–9].

To scrutinize the LDME universality is an ongoing task. Currently, these tests are performed at next-to-leading order (NLO) in the strong coupling constant α_s , and may, for LDMEs concerning J/ψ , be summarized as follows: The LDMEs of the global fit [10] to 194 points of J/ψ production data in pp , $p\bar{p}$, γp , $\gamma\gamma$ and e^+e^- scattering describe the fitted observables reasonably well, but result in discrepancies for η_c [11] and $J/\psi + W$ or Z [12] yields at the LHC, and predict strong transverse J/ψ polarization, not observed at Tevatron or the LHC [13]. All other LDME fits are restricted to high transverse momentum p_T hadroproduction data, with low- p_T cuts of typically 7 GeV or higher [3, 4, 14–18]. They are successful at describing the fitted high p_T yields and the measured J/ψ polarization, but describe neither the hadroproduction data at lower p_T nor the inelasticity variable z integrated photoproduction [19], and the $J/\psi + W$ or Z data [20–22] at best marginally [12]. η_c hadroproduction is almost exclusively determined by $\langle \mathcal{O}^{J/\psi}({}^1S_0^{[8]}) \rangle$. The fit results of Refs. [3, 4, 14] leave $\langle \mathcal{O}^{J/\psi}({}^1S_0^{[8]}) \rangle$ poorly constrained, predicting η_c production therefore only with very large uncertainties. On the other hand, Refs. [15, 18] lead to an overshoot of η_c data. Only analyses [16, 17] describe η_c production well, because they use LHCb η_c data directly as input to constrain $\langle \mathcal{O}^{J/\psi}({}^1S_0^{[8]}) \rangle$. The latter approach thus appears to be the most promising fit strategy, and is the one we adopt in the analysis described here.

In our NLO analysis, we fit the three J/ψ CO LDMEs to prompt LHCb η_c [23, 24] and CMS J/ψ [25] production yields, the latter data ranging from $p_T = 10$ GeV to 120 GeV. After showing that these LDMEs lead to a good description of the CMS J/ψ polarization data [25], we go on to make predictions for observables never studied in this context before: We show that our LDMEs can predict well recent ATLAS J/ψ hadroproduction data with p_T ranging up to 360 GeV [26] in contrast with recent finding that the cross section turns

negative at very large p_T [27]. We further show that, contrary to a common perception, these fits can well describe J/ψ photoproduction at HERA [28, 29] even at p_T as low as 1 GeV, as long as we consider the region $z < 0.6$. Also, $\gamma\gamma$ scattering at LEP [30] can be well described down to $p_T = 1$ GeV. Even $\Upsilon(nS)$ production [31] is well reproduced, while $J/\psi + Z$ production [21] remains intricate to be interpreted. All these findings are nontrivial tests of NRQCD factorization never performed before.

This analysis also provides a technological advancement: We develop and apply a consistent fit-and-predict procedure, which for the first time systematically takes into account the effect of scale variations, the largest source of uncertainty of the SDCs. In most NRQCD analyses, e.g. Refs. [14–17], scale variations are simply ignored. In Refs. [10–13, 19, 32–36], scale uncertainties are considered in predictions and plots, but, unrealistically, assumed to be uncorrelated to the LDME errors, leading to unnecessarily large error bands. In the analyses [3, 4, 18], scale uncertainties are treated as global theory errors in the fits. But then, even if scale uncertainties were indeed global and independent of e.g. p_T , the LDME fit errors obtained in this way would still not be sufficient to predict scale uncertainties of other observables, which have their own individual scale dependencies. Therefore, in our analysis, we proceed as follows. We do three separate fits, with the renormalization and factorization scales μ_r and μ_f set equal and equal to $\mu_0/2$, μ_0 and $2\mu_0$, respectively, with μ_0 our default hard scale. For prediction plots, we then create three error bands, each created using the LDME uncertainties of one fit, in combination with the SDCs evaluated with the respective scale choice. Our overall uncertainty is then the envelope of the three error bands created this way. This procedure takes into account correlations between fit errors and scale uncertainties, while at the same time acknowledging the individual scale dependencies of the various observables.

2 Details and input of the calculation

We calculate the SDCs needed for hadroproduction yields using the dipole subtraction based codes described in Refs. [12, 37, 38]. For J/ψ polarization and for J/ψ production in γp and $\gamma\gamma$ scattering, we calculate the SDCs using the phase-space slicing [39] based codes described in Refs. [10, 13, 38, 40]. We use three (four) light quark flavours for charmonia (bottomonia) in loops and external legs, heavy quarks only for the outgoing $Q\bar{Q}$ pair. We set the default hard scale to be $\mu_0 = m_T = (p_T^2 + 4m_Q^2)^{1/2}$, the quarkonium transverse mass, and the NRQCD scale to be $\mu_\Lambda = m_Q$. We choose the on-shell charm and bottom masses to be $m_c = 1.5$ GeV and $m_b = 4.75$ GeV. As proton parton distribution function (PDF) set, we use CTEQ6M [41], and for $\alpha_s(\mu_r)$ correspondingly the two loop running formula with the asymptotic scale parameter $\Lambda_{\text{QCD}}^{(n_f=4)} = 326$ MeV ($\Lambda_{\text{QCD}}^{(n_f=5)} = 226$ MeV) for charmonia (bottomonia). In γp and $\gamma\gamma$ scattering, we use the Weizsäcker–Williams approximation for the photon flux and for resolved photons the AFG04.BF PDF set [42]. We evaluate $\psi(2S) \rightarrow J/\psi$ feeddown assuming $p_{T,\psi(2S)}/p_{T,J/\psi} = m_{\psi(2S)}/m_{J/\psi} = 1.19$ [43]. The $\chi_{cJ} \rightarrow J/\psi$ feeddown contributions are estimated for J/ψ hadroproduction by interpolating ATLAS data [44], and for $J/\psi + Z$ production to be 20% of the direct $^3S_1^{[8]}$

	$\langle \mathcal{O}^{J/\psi}(^3S_1^{[8]}) \rangle$	$\langle \mathcal{O}^{J/\psi}(^1S_0^{[8]}) \rangle$	$\langle \mathcal{O}^{J/\psi}(^3P_0^{[8]}) \rangle / m_c^2$	$\chi_{\min}^2/\text{d.o.f}$
$\mu_r = \mu_f = m_T/2$	0.604 ± 0.106	-0.501 ± 0.171	0.716 ± 0.169	0.26
$\mu_r = \mu_f = m_T$	1.062 ± 0.195	-0.204 ± 0.229	1.905 ± 0.422	0.18
$\mu_r = \mu_f = 2m_T$	1.367 ± 0.261	0.094 ± 0.288	3.232 ± 0.732	0.15

Table 1: Fit results in units of 10^{-2} GeV^3 for our three scale choices $\mu_r = \mu_f = m_T/2$, m_T and $2m_T$.

production channel, based on Ref. [12] and the fitted value of $\langle \mathcal{O}^{\chi_{c0}}(^3S_1^{[8]}) \rangle$ in Ref. [45]. We neglect χ_{cJ} feeddowns for our polarization predictions due to their small influence on λ_θ [4], and in γp and $\gamma\gamma$ scattering due to their smallness there [28–30]. $\chi_{bJ} \rightarrow \Upsilon(nS)$ feeddowns are estimated by using the LHCb measured feeddown fractions [46]. $h_c \rightarrow \eta_c$ feeddown is again negligible [11] and neglected, too. We adopt the values for all branching fractions from Ref. [43]. Our fits are standard least-square fits of the three parameters $\langle \mathcal{O}^{J/\psi}(^3S_1^{[8]}) \rangle$, $\langle \mathcal{O}^{J/\psi}(^1S_0^{[8]}) \rangle$ and $\langle \mathcal{O}^{J/\psi}(^3P_0^{[8]}) \rangle / m_c^2$, in this order, taking into account experimental errors and a global 30% theory error due to unknown relativistic corrections. We relate our fit parameters to the three η_c CO LDMEs via HQSS relations [1], and to the $\psi(2S)$ and $\Upsilon(nS)$ CO LDMEs according to the pNRQCD derived relations (3.47)–(3.48) of Ref. [4]. The CS LDMEs are not fitted, but fixed as $\langle \mathcal{O}^{J/\psi}(^3S_1^{[1]}) \rangle = 1.16 \text{ GeV}^3$ [47], $\langle \mathcal{O}^{\psi(2S)}(^3S_1^{[1]}) \rangle = 0.76 \text{ GeV}^3$ [47], $\langle \mathcal{O}^{\Upsilon(3S)}(^3S_1^{[1]}) \rangle = 3.54 \text{ GeV}^3$ [47] and $\langle \mathcal{O}^{\eta_c}(^1S_0^{[1]}) \rangle = 0.328 \text{ GeV}^3$ [48].

3 Fit results

The best-fit values and the χ_{\min}^2 per degree of freedom (d.o.f.) of our three fits are listed in Table 1. The respective correlation matrices are

$$C_{m_T/2} = \begin{pmatrix} 1.113 & -0.407 & 1.764 \\ -0.407 & 2.925 & -0.592 \\ 1.764 & -0.592 & 2.839 \end{pmatrix} \times 10^{-6} \text{ GeV}^6, \quad (1)$$

$$C_{m_T} = \begin{pmatrix} 3.819 & -1.383 & 8.222 \\ -1.383 & 5.255 & -2.875 \\ 8.222 & -2.875 & 17.818 \end{pmatrix} \times 10^{-6} \text{ GeV}^6, \quad (2)$$

$$C_{2m_T} = \begin{pmatrix} 6.831 & -2.848 & 19.092 \\ -2.848 & 8.322 & -7.788 \\ 19.092 & -7.788 & 53.638 \end{pmatrix} \times 10^{-6} \text{ GeV}^6. \quad (3)$$

In Fig. 1, we compare the theoretical predictions using our fit results to the 42 data points. The central values are drawn by solid black lines and the uncertainties by colored bands, whereby the overall uncertainties are given by the yellow bands and the uncertainties only of the central fit by the orange bands inside them. We will use this convention for all plots throughout this publication. The level of agreement to the data apparent from Fig. 1 is in line with the very low values of $\chi_{\min}^2/\text{d.o.f}$ in Table 1. The Fock state decomposition

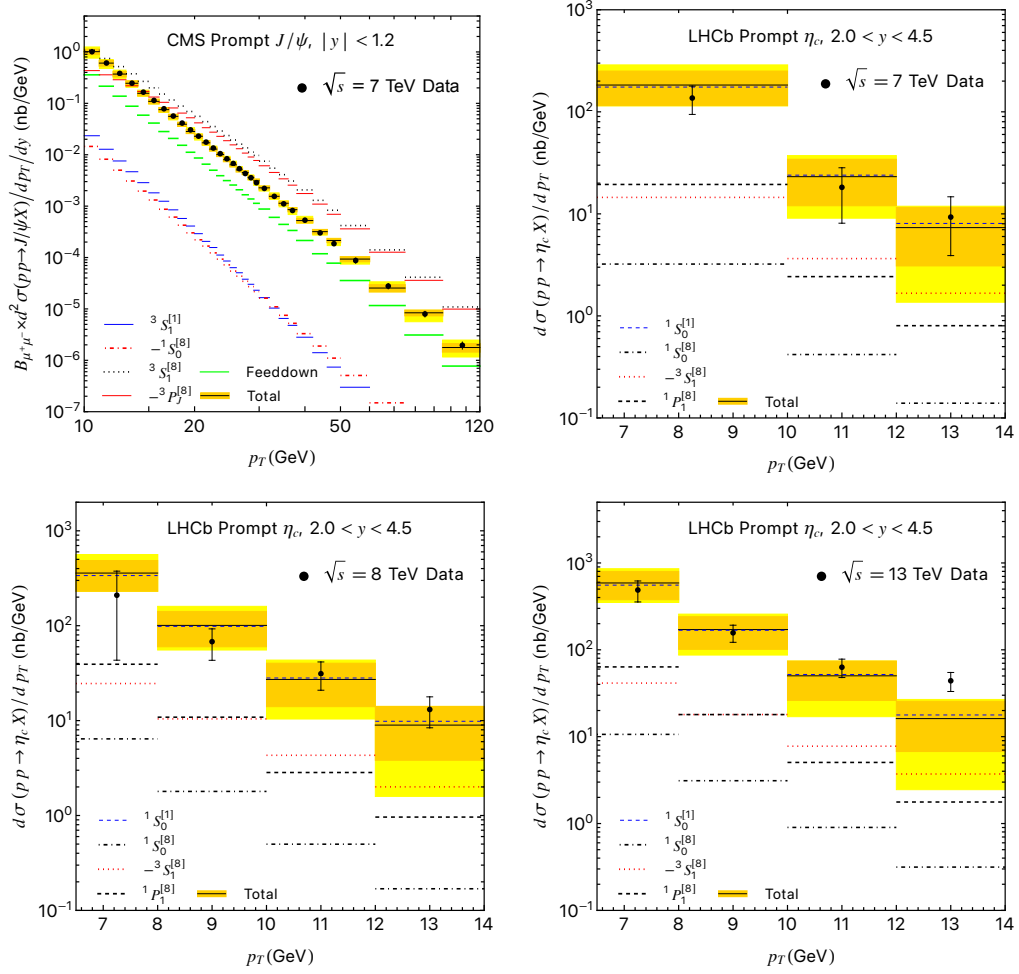


Figure 1: Predictions for prompt J/ψ production at CMS [25] and η_c production at LHCb [23, 24]. The data shown is exactly the data used for the LDME fits. The total cross section is broken down into feeddown contributions and the direct contributions of the individual Fock states. The uncertainty bands are as described in the main text.

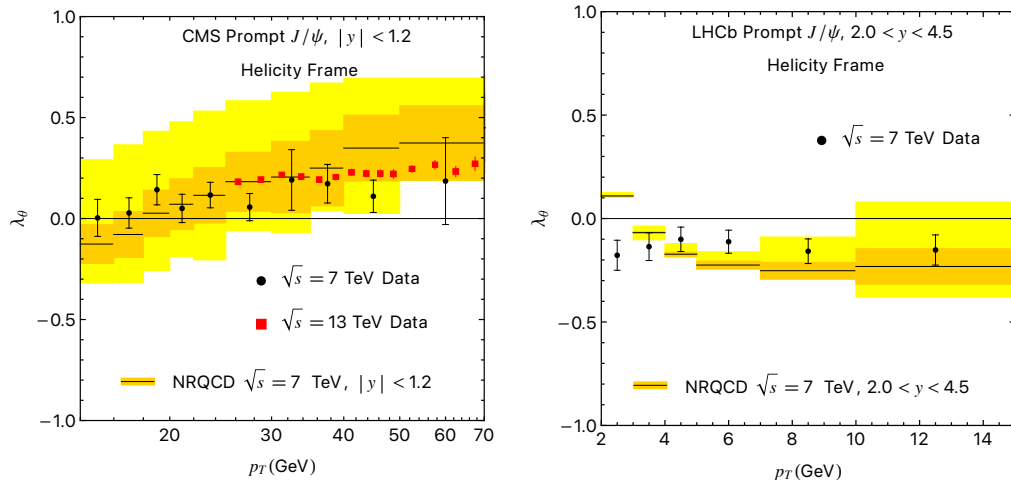


Figure 2: Theory predictions for the J/ψ polarization parameter λ_θ in the helicity frame compared to CMS [49, 50] and LHCb [51] data. The total cross sections are broken down into feeddown contributions and the direct contributions of the individual Fock states. The uncertainty bands are as described in the main text.

shows the familiar features [16,17] of the high p_T J/ψ and η_c fit: On the one hand, it is based on the cancellation between a large positive ${}^3S_1^{[8]}$ and a large negative ${}^3P_J^{[8]}$ J/ψ production channel. We note here that this cancellation is not a fine-tuning problem, because NLO LDME mixing implies that only the sum of both contributions has physical significance, see e.g. section 3.2 of Ref. [37] for more details. On the other hand, $\langle \mathcal{O}^{J/\psi}({}^1S_0^{[8]}) \rangle \approx \langle \mathcal{O}^{\eta_c}({}^3S_1^{[8]}) \rangle$ is almost solely determined via η_c production: With η_c data already exhausted by the CS contribution, $\langle \mathcal{O}^{J/\psi}({}^1S_0^{[8]}) \rangle$ is restricted to very small values.

4 Predictions

J/ψ polarization — Fig. 2 shows our predictions for the J/ψ polarization parameter λ_θ in the helicity frame, compared to CMS [49, 50] and LHCb [51] data. Our predictions are in good agreement with these measurements and match the pattern that λ_θ turns from slightly negative at relatively low p_T to positive and converges to $\lambda_\theta \sim 0.3$ at high p_T . No J/ψ polarization puzzle appears here.

J/ψ hadroproduction at very high p_T — The recent ATLAS measurement [26] of the J/ψ p_T differential distribution at $\sqrt{s} = 13$ TeV with p_T ranging up to 360 GeV has received significant attention. In the publication itself, data was compared to NLO NRQCD predictions using LDME input from Ref. [10]. Although there were no unreasonable discrepancies, theory errors were expectedly large at these very high p_T values with their dominating $\log(m_c^2/p_T^2)$ terms. Leading power resummations of these $\log(m_c^2/p_T^2)$ contributions have indeed been shown to yield a significant effect [18, 53, 54]. Ref. [27] later

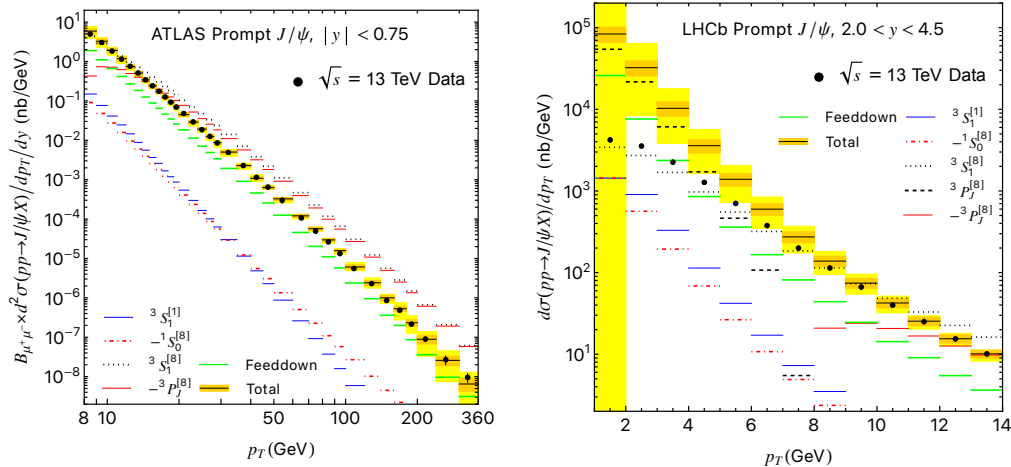


Figure 3: The predictions for J/ψ hadroproduction measured by ATLAS [26] and LHCb [52]. The total cross sections are broken down into feeddown contributions and the direct contributions of the individual Fock states. The uncertainty bands are as described in the main text.

showed that NLO NRQCD predictions with LDME input from Refs. [3, 4] turned predictions negative at large p_T . With these expectations in mind, it appears surprising that our predictions of the η_c and J/ψ combined fit, which we show in the left panel of Fig. 3, exhibit instead a very good description of that data, even up to the highest measured p_T values.

J/ψ hadroproduction at low p_T — In the right panel of Fig. 3, we compare our predictions to J/ψ production data from LHCb [52], reaching down to $p_T = 1$ GeV. Here, we recover the feature familiar from other high p_T fits [3, 4, 14–18] that low p_T data is not reproduced. The reason is that the ${}^3P_J^{[8]}$ SDCs change sign from negative to positive when going below $p_T \approx 7$ GeV, so that instead of a cancellation between ${}^3S_1^{[8]}$ and ${}^3P_J^{[8]}$ channels there is an amplification. The resulting steep increase at low p_T is not observed in the data.

$\Upsilon(nS)$ hadroproduction — The left panel of Fig. 4 shows our predictions for the p_T differential $\Upsilon(3S)$ production measured by ATLAS [31]. These results are a genuine prediction of the equations (3.47)–(3.48) of Ref. [4] derived from pNRQCD, which relate $\Upsilon(3S)$ to the J/ψ CO LDMEs. The accurate description of the data seen can thus also be viewed as a highly nontrivial confirmation of the pNRQCD relations, the more so as scale evolutions in equation (3.47) of Ref. [4] result in a very different Fock state decomposition in $\Upsilon(3S)$ as compared to J/ψ production. In particular, there is no strong cancellation between ${}^3S_1^{[8]}$ and ${}^3P_J^{[8]}$ channels here. Instead, the cross section decomposes almost equally into the ${}^3S_1^{[8]}$ channel and feeddown from χ_{bJ} mesons. For $\Upsilon(1S)$ and $\Upsilon(2S)$, we reach

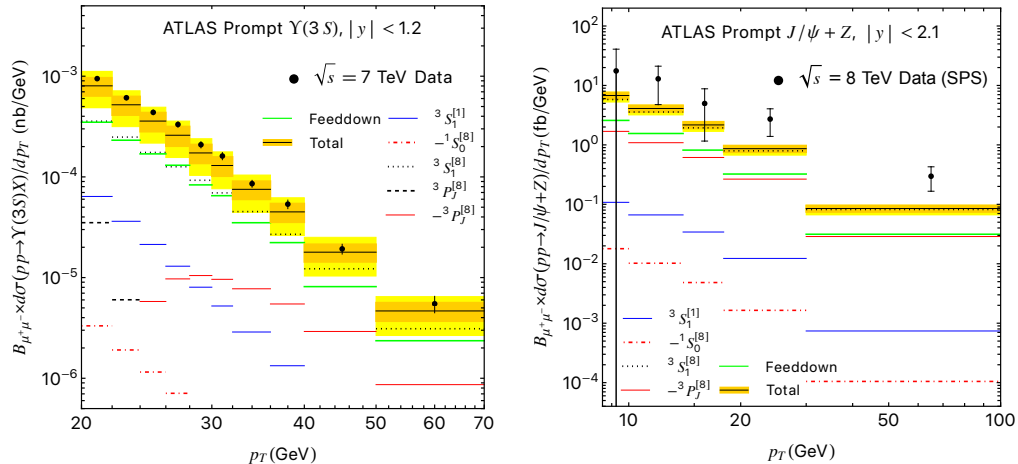


Figure 4: The predictions for $\Upsilon(3S)$ [31] and $J/\psi + Z$ [21] production measured by ATLAS. For the $J/\psi + Z$ data shown in the plot, we have subtracted the DPS contributions estimated in Ref. [21] using the DPS effective area value $\sigma_{\text{eff}} = 15^{+5.8}_{-4.2}$ mb of Ref. [55]. The total cross sections are broken down into feeddown contributions and the direct contributions of the individual Fock states. The uncertainty bands are as described in the main text.

similar conclusions.

LHCb $J/\psi + Z$ production — In the right panel of Fig. 4, we show our predictions for $J/\psi + Z$ production measured by ATLAS [21], where estimated double parton scattering (DPS) contributions are already subtracted from the data. The predictions are dominated by the $^3S_1^{[8]}$ channel. For the two highest p_T bins, predictions lie around two experimental standard deviations below data. Given the fact that in Ref. [21], a data-driven analysis of the J/ψ - Z angular distribution confirmed single parton scattering (SPS) dominance, it appears unlikely, albeit not impossible, that the discrepancy is due to underestimated DPS contributions.

J/ψ production in $\gamma\gamma$ scattering — In Fig. 5a, we show predictions for p_T^2 differential J/ψ production in $\gamma\gamma$ scattering at LEP DELPHI [30], in the range $1 \text{ GeV}^2 < p_T^2 < 10 \text{ GeV}^2$. Contrary to the hadroproduction case, this low p_T data is reasonably well described, even though the very low statistics of the measurement does not allow for more than an order-of-magnitude comparison. We note that the cross sections are almost exclusively given by single-resolved photon contributions.

J/ψ production in HERA photoproduction — In Figs. 5b–5f, we show our predictions for p_T^2 differential J/ψ photoproduction at HERA [28, 29] for five bins of the inelasticity variable z , which measures in the proton rest frame the fraction of photon

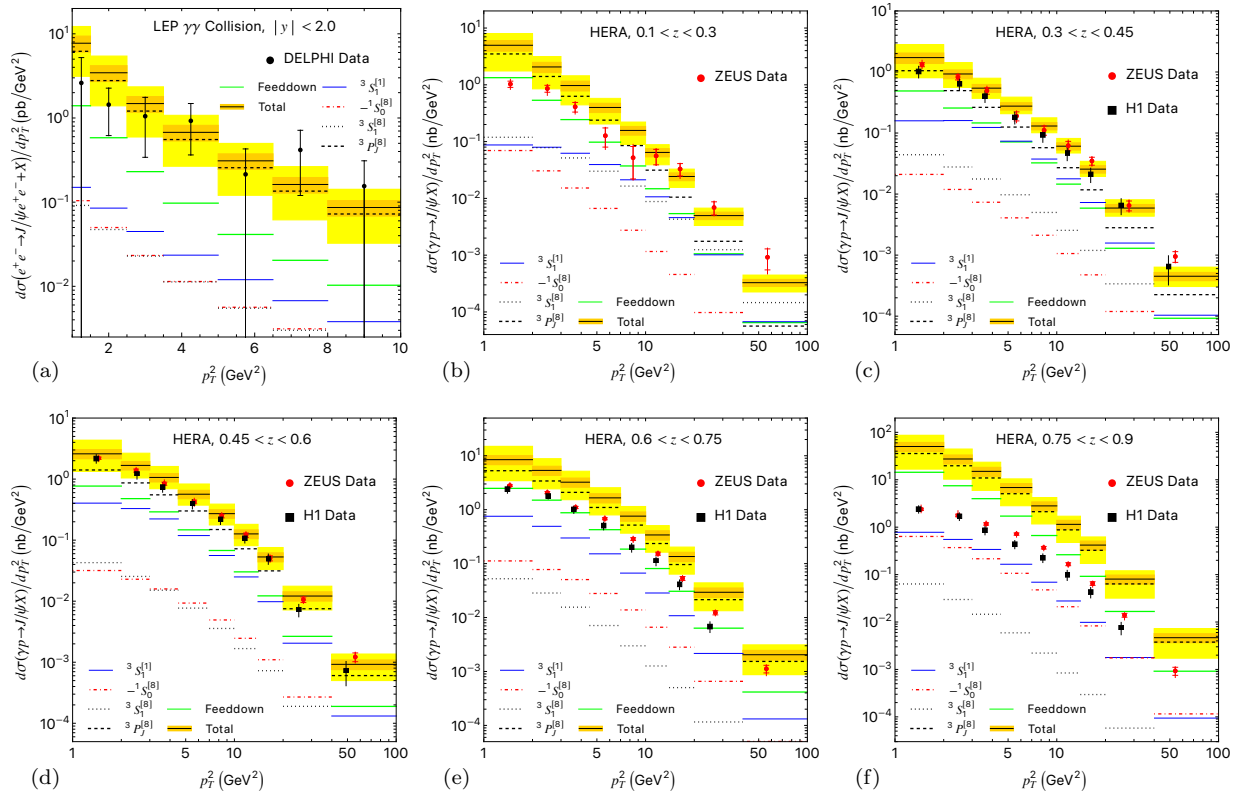


Figure 5: The predictions for p_T^2 differential cross sections of J/ψ production compared to DELPHI [30] two photon collision data at LEP (a) and HERA photoproduction data measured by H1 [28] and ZEUS [29] (b–f). The LEP predictions are evaluated with a center-of-mass energy $\sqrt{s} = 197$ GeV, rapidity y range $|y| < 2$, photon center-of-mass energy $W < 35$ GeV and an electron scattering angle $\theta_{el} < 32$ mrad, in line with the experimental setup. The predictions for HERA are evaluated with $\sqrt{s} = 317$ GeV, a photon virtuality squared $Q^2 < 1$ GeV² and a photon-proton center-of-mass energy range $60 \text{ GeV} < W < 240$ GeV, corresponding to the ZEUS [29] experimental setup. The H1 analysis [28] uses the same parameters, except for the Q^2 range, which is $Q^2 < 2.5$ GeV² there. To compare with the γp HERA data, we divide the calculated e^+e^- cross sections by the averaged photon flux 0.1024 [28]. The total cross sections are broken down into feeddown contributions and the direct contributions of the individual Fock states. All curves show the sum of non-, single- (and double-) resolved photon contributions, which are not broken down here, to avoid clutter. The uncertainty bands are as described in the main text.

energy transferred to the J/ψ . In the region $0.1 < z < 0.3$ with $p_T^2 < 40 \text{ GeV}^2$, resolved photons are dominating our predictions, while for the other regions, nonresolved photons are dominating. We recover the increase of the cross section at $z \rightarrow 1$, known e.g. from Fig. 3.3 of Ref. [56], which is not observed in the data. For $0.75 < z < 0.9$, predictions overshoot the data by factors of 5.2 to 20. Surprisingly, in the $z < 0.6$ regions, we obtain a good description of the data over the whole measured p_T range, again down to $p_T = 1 \text{ GeV}$, with a significant deviation only for the low p_T end of the lowest z bin, which coincides with the region where resolved photoproduction dominates.

5 Discussion and summary

Although NLO predictions of the high p_T J/ψ plus η_c combined fit presented here lead to many nontrivial descriptions of various quarkonium production data, discrepancies remain. Moreover, these discrepancies are not at places where one would naively expect them. A naive expectation would be that fixed order NLO calculations may fail at $p_T^2 \gg 4m_Q^2$ and in the endpoint regions $p_T^2 \ll 4m_Q^2$ and $1 - z \ll 1$, where large logarithms spoil the perturbative convergence. The hadroproduction predictions from the LDME fit presented here are, however, very good for $p_T^2 \gg 4m_Q^2$, but fail in the region $p_T^2 \lesssim 4m_Q^2$. On the other hand, the latter region works well for $z < 0.6$ HERA photoproduction, while for $z > 0.6$, HERA data is not described, regardless of p_T . LDME universality thus remains in question. It is, however, noticeable that the regions of disagreement $p_T^2 \lesssim 4m_Q^2$ and $z > 0.6$ coincide with “extensions” of endpoint regions, for which solutions, e.g. via nonperturbative shape functions [57–59], have been proposed. The questions as to why there is no disagreement for $p_T^2 \gg 4m_Q^2$, and why the $p_T^2 \lesssim 4m_Q^2$ discrepancy does not appear in low z photoproduction, remain, however, to be explained.

To summarize, we have done a combined fit of the three J/ψ CO LDMEs to 42 data points of CMS J/ψ and LHCb η_c production data and made predictions for CMS and LHCb J/ψ polarization, ATLAS high p_T J/ψ production, ATLAS $\Upsilon(nS)$ and $J/\psi + Z$ production, LHCb low p_T J/ψ production as well as J/ψ production in $\gamma\gamma$ collisions at LEP and γp collisions at HERA. We have thereby used a novel fit-and-predict procedure, which systematically takes into account the effect of scale variations. The predictions show good agreement with data everywhere with the exception of low and medium p_T hadroproduction, HERA photoproduction at $z > 0.6$, and possibly the two highest LHCb $J/\psi + Z$ production bins. In particular, our findings for J/ψ production in $\gamma\gamma$ and γp scattering may be of significance for future quarkonium studies, in particular at the EIC and the high-luminosity LHC.

Acknowledgments — X.-P. W would like to thank A. Bruni and H.-S Shao for useful discussions. We thank A. Vairo for reading the paper and giving very useful comments. The work of N. B. and X.-P. W. is supported by the DFG (Deutsche Forschungsgemeinschaft, German Research Foundation) Grant No. BR 4058/2-2. We acknowledge support from the DFG cluster of excellence “ORIGINS” under Germany’s Excellence Strategy - EXC-

2094 - 390783311. X.-P. W. acknowledges support from STRONG-2020- European Union’s Horizon 2020 research and innovation program under grant agreement No. 824093. N. B. acknowledges the European Union ERC-2023-ADG- Project EFT-XYZ. The work of M. B. is supported by the German Research Foundation DFG through Grant No. BU 3455/1-1. The authors would like to express special thanks to the Mainz Institute for Theoretical Physics (MITP) of the Cluster of Excellence PRISMA+ (Project ID 390831469), for its hospitality and support.

References

- [1] Geoffrey T. Bodwin, Eric Braaten, and G. Peter Lepage. Rigorous QCD analysis of inclusive annihilation and production of heavy quarkonium. *Phys. Rev.*, D51:1125–1171, 1995. [Erratum: *Phys. Rev. D* 55, 5853 (1997)].
- [2] G. Peter Lepage, Lorenzo Magnea, Charles Nakhleh, Ulrika Magnea, and Kent Hornbostel. Improved nonrelativistic QCD for heavy quark physics. *Phys. Rev. D*, 46:4052–4067, 1992.
- [3] Nora Brambilla, Hee Sok Chung, Antonio Vairo, and Xiang-Peng Wang. Production and polarization of S-wave quarkonia in potential nonrelativistic QCD. *Phys. Rev. D*, 105(11):L111503, 2022.
- [4] Nora Brambilla, Hee Sok Chung, Antonio Vairo, and Xiang-Peng Wang. Inclusive production of J/ψ , $\psi(2S)$, and Υ states in pNRQCD. *JHEP*, 03:242, 2023.
- [5] A. Pineda and J. Soto. Effective field theory for ultrasoft momenta in NRQCD and NRQED. *Nucl. Phys. B Proc. Suppl.*, 64:428–432, 1998.
- [6] Nora Brambilla, Antonio Pineda, Joan Soto, and Antonio Vairo. Potential NRQCD: An Effective theory for heavy quarkonium. *Nucl. Phys.*, B566:275, 2000.
- [7] Nora Brambilla, Antonio Pineda, Joan Soto, and Antonio Vairo. Effective Field Theories for Heavy Quarkonium. *Rev. Mod. Phys.*, 77:1423, 2005.
- [8] Nora Brambilla, Hee Sok Chung, and Antonio Vairo. Inclusive Hadroproduction of P -Wave Heavy Quarkonia in Potential Nonrelativistic QCD. *Phys. Rev. Lett.*, 126(8):082003, 2021.
- [9] Nora Brambilla, Hee Sok Chung, and Antonio Vairo. Inclusive production of heavy quarkonia in pNRQCD. *JHEP*, 09:032, 2021.
- [10] Mathias Butenschoen and Bernd A. Kniehl. World data of J/ψ production consolidate NRQCD factorization at NLO. *Phys. Rev. D*, 84:051501, 2011.
- [11] Mathias Butenschoen, Zhi-Guo He, and Bernd A. Kniehl. η_c production at the LHC challenges nonrelativistic-QCD factorization. *Phys. Rev. Lett.*, 114(9):092004, 2015.

- [12] Mathias Butenschoen and Bernd A. Kniehl. Constraints on Nonrelativistic-QCD Long-Distance Matrix Elements from J/ψ Plus W/Z Production at the LHC. *Phys. Rev. Lett.*, 130(4):041901, 2023.
- [13] Mathias Butenschoen and Bernd A. Kniehl. J/ψ polarization at Tevatron and LHC: Nonrelativistic-QCD factorization at the crossroads. *Phys. Rev. Lett.*, 108:172002, 2012.
- [14] Yan-Qing Ma, Kai Wang, and Kuang-Ta Chao. $J/\psi(\psi')$ production at the Tevatron and LHC at $\mathcal{O}(\alpha_s^4 v^4)$ in nonrelativistic QCD. *Phys. Rev. Lett.*, 106:042002, 2011.
- [15] Bin Gong, Lu-Ping Wan, Jian-Xiong Wang, and Hong-Fei Zhang. Polarization for Prompt J/ψ and $\psi(2s)$ Production at the Tevatron and LHC. *Phys. Rev. Lett.*, 110(4):042002, 2013.
- [16] Hao Han, Yan-Qing Ma, Ce Meng, Hua-Sheng Shao, and Kuang-Ta Chao. η_c production at LHC and indications on the understanding of J/ψ production. *Phys. Rev. Lett.*, 114(9):092005, 2015.
- [17] Hong-Fei Zhang, Zhan Sun, Wen-Long Sang, and Rong Li. Impact of η_c hadroproduction data on charmonium production and polarization within NRQCD framework. *Phys. Rev. Lett.*, 114(9):092006, 2015.
- [18] Geoffrey T. Bodwin, Kuang-Ta Chao, Hee Sok Chung, U-Rae Kim, Jungil Lee, and Yan-Qing Ma. Fragmentation contributions to hadroproduction of prompt J/ψ , χ_{cJ} , and $\psi(2S)$ states. *Phys. Rev. D*, 93(3):034041, 2016.
- [19] Mathias Butenschoen and Bernd A. Kniehl. Next-to-leading-order tests of NRQCD factorization with J/ψ yield and polarization. *Mod. Phys. Lett. A*, 28:1350027, 2013.
- [20] Georges Aad et al. Measurement of the production cross section of prompt J/ψ mesons in association with a W^\pm boson in pp collisions at $\sqrt{s} = 7$ TeV with the ATLAS detector. *JHEP*, 04:172, 2014.
- [21] Georges Aad et al. Observation and measurements of the production of prompt and non-prompt J/ψ mesons in association with a Z boson in pp collisions at $\sqrt{s} = 8$ TeV with the ATLAS detector. *Eur. Phys. J. C*, 75(5):229, 2015.
- [22] Morad Aaboud et al. Measurement of J/ψ production in association with a W^\pm boson with pp data at 8 TeV. *JHEP*, 01:095, 2020.
- [23] Roel Aaij et al. Measurement of the $\eta_c(1S)$ production cross-section in proton-proton collisions via the decay $\eta_c(1S) \rightarrow p\bar{p}$. *Eur. Phys. J. C*, 75(7):311, 2015.
- [24] Roel Aaij et al. Study of charmonium production via the decay to $p\bar{p}$ at $\sqrt{s} = 13\text{TeV}$. 7 2024.

- [25] Vardan Khachatryan et al. Measurement of J/ψ and $\psi(2S)$ Prompt Double-Differential Cross Sections in pp Collisions at $\sqrt{s}=7$ TeV. *Phys. Rev. Lett.*, 114(19):191802, 2015.
- [26] Georges Aad et al. Measurement of the production cross-section of J/ψ and $\psi(2S)$ mesons in pp collisions at $\sqrt{s} = 13$ TeV with the ATLAS detector. *Eur. Phys. J. C*, 84(2):169, 2024.
- [27] Hee Sok Chung, U-Rae Kim, and Jungil Lee. Resummation of threshold double logarithms in hadroproduction of heavy quarkonium. 8 2024.
- [28] F. D. Aaron et al. Inelastic Production of J/ψ Mesons in Photoproduction and Deep Inelastic Scattering at HERA. *Eur. Phys. J. C*, 68:401–420, 2010.
- [29] H. Abramowicz et al. Measurement of inelastic J/ψ and ψ' photoproduction at HERA. *JHEP*, 02:071, 2013.
- [30] J. Abdallah et al. Study of inclusive J/ψ production in two photon collisions at LEP-2 with the DELPHI detector. *Phys. Lett. B*, 565:76–86, 2003.
- [31] Georges Aad et al. Measurement of Upsilon production in 7 TeV pp collisions at ATLAS. *Phys. Rev. D*, 87(5):052004, 2013.
- [32] Mathias Butenschoen and Bernd A. Kniehl. Global analysis of $\psi(2S)$ inclusive hadroproduction at next-to-leading order in nonrelativistic-QCD factorization. *Phys. Rev. D*, 107(3):034003, 2023.
- [33] Mathias Butenschoen and Bernd A. Kniehl. Probing nonrelativistic QCD factorization in polarized J/ψ photoproduction at next-to-leading order. *Phys. Rev. Lett.*, 107:232001, 2011.
- [34] Mathias Butenschoen and Bernd A. Kniehl. Reconciling J/ψ production at HERA, RHIC, Tevatron, and LHC with NRQCD factorization at next-to-leading order. *Phys. Rev. Lett.*, 106:022003, 2011.
- [35] Mathias Butenschoen, Zhi-Guo He, and Bernd A. Kniehl. Deciphering the $X(3872)$ via its polarization in prompt production at the CERN LHC. *Phys. Rev. Lett.*, 123(3):032001, 2019.
- [36] Mathias Butenschoen, Zhi-Guo He, and Bernd A. Kniehl. NLO NRQCD disfavors the interpretation of $X(3872)$ as $\chi_{c1}(2P)$. *Phys. Rev. D*, 88:011501, 2013.
- [37] Mathias Butenschoen and Bernd A. Kniehl. Dipole subtraction at next-to-leading order in nonrelativistic-QCD factorization. *Nucl. Phys. B*, 950:114843, 2020.
- [38] Mathias Butenschoen and Bernd A. Kniehl. Dipole Subtraction vs. Phase Space Slicing in NLO NRQCD Heavy-Quarkonium Production Calculations. *Nucl. Phys. B*, 957:115056, 2020.

- [39] B. W. Harris and J. F. Owens. The Two cutoff phase space slicing method. *Phys. Rev. D*, 65:094032, 2002.
- [40] Mathias Butenschoen and Bernd A. Kniehl. Complete next-to-leading-order corrections to J/ψ photoproduction in nonrelativistic quantum chromodynamics. *Phys. Rev. Lett.*, 104:072001, 2010.
- [41] J. Pumplin, D. R. Stump, J. Huston, H. L. Lai, Pavel M. Nadolsky, and W. K. Tung. New generation of parton distributions with uncertainties from global QCD analysis. *JHEP*, 07:012, 2002.
- [42] P. Aurenche, M. Fontannaz, and J. Ph. Guillet. New NLO parametrizations of the parton distributions in real photons. *Eur. Phys. J. C*, 44:395–409, 2005.
- [43] S. Navas et al. Review of particle physics. *Phys. Rev. D*, 110(3):030001, 2024.
- [44] Georges Aad et al. Measurement of χ_{c1} and χ_{c2} production with $\sqrt{s} = 7$ TeV pp collisions at ATLAS. *JHEP*, 07:154, 2014.
- [45] Yan-Qing Ma, Kai Wang, and Kuang-Ta Chao. QCD radiative corrections to χ_{cJ} production at hadron colliders. *Phys. Rev. D*, 83:111503, 2011.
- [46] Roel Aaij et al. Study of χ_b meson production in $p p$ collisions at $\sqrt{s} = 7$ and 8 TeV and observation of the decay $\chi_b(3P) \rightarrow \Upsilon(3S)\gamma$. *Eur. Phys. J. C*, 74(10):3092, 2014.
- [47] Estia J. Eichten and Chris Quigg. Quarkonium wave functions at the origin. *Phys. Rev. D*, 52:1726–1728, 1995.
- [48] Geoffrey T. Bodwin, Hee Sok Chung, Daekyoung Kang, Jungil Lee, and Chaehyun Yu. Improved determination of color-singlet nonrelativistic QCD matrix elements for S-wave charmonium. *Phys. Rev. D*, 77:094017, 2008.
- [49] Serguei Chatrchyan et al. Measurement of the Prompt J/ψ and $\psi(2S)$ Polarizations in pp Collisions at $\sqrt{s} = 7$ TeV. *Phys. Lett. B*, 727:381–402, 2013.
- [50] Aram Hayrapetyan et al. Measurement of the polarizations of prompt and non-prompt J/ψ and $\psi(2S)$ mesons produced in pp collisions at $\sqrt{s} = 13$ TeV. 6 2024.
- [51] R Aaij et al. Measurement of J/ψ polarization in pp collisions at $\sqrt{s} = 7$ TeV. *Eur. Phys. J. C*, 73(11):2631, 2013.
- [52] Roel Aaij et al. Measurement of forward J/ψ production cross-sections in pp collisions at $\sqrt{s} = 13$ TeV. *JHEP*, 10:172, 2015. [Erratum: *JHEP* 05, 063 (2017)].
- [53] Zhong-Bo Kang, Yan-Qing Ma, Jian-Wei Qiu, and George Sterman. Heavy Quarkonium Production at Collider Energies: Factorization and Evolution. *Phys. Rev. D*, 90(3):034006, 2014.

- [54] Geoffrey T. Bodwin, Hee Sok Chung, U-Rae Kim, and Jungil Lee. Fragmentation contributions to J/ψ production at the Tevatron and the LHC. *Phys. Rev. Lett.*, 113(2):022001, 2014.
- [55] Georges Aad et al. Measurement of hard double-parton interactions in $W(\rightarrow l\nu)+2$ jet events at $\sqrt{s}=7$ TeV with the ATLAS detector. *New J. Phys.*, 15:033038, 2013.
- [56] Daniël Boer et al. Physics case for quarkonium studies at the Electron Ion Collider. 9 2024.
- [57] M. Beneke, I. Z. Rothstein, and Mark B. Wise. Kinematic enhancement of nonperturbative corrections to quarkonium production. *Phys. Lett. B*, 408:373–380, 1997.
- [58] Sean Fleming, Adam K. Leibovich, and Thomas Mehen. Resummation of Large Endpoint Corrections to Color-Octet J/ψ Photoproduction. *Phys. Rev. D*, 74:114004, 2006.
- [59] Yan-Qing Ma and Kuang-Ta Chao. New factorization theory for heavy quarkonium production and decay. *Phys. Rev. D*, 100(9):094007, 2019.